Millimeter Wave Phase Measurement using EO Sampling Method

Yukiyasu Kimura, Takashi Mori, Masaaki Fuse, Shigenori Mattori

[Summary] The huge increase in mobile data traffic requires use of the millimeter waveband to implement transmission speeds of several Gbps. However it is difficult to accurately evaluate wideband signals using this waveband. Since measurement systems using down converters include the frequency characteristics of the system in the measured value, accurate evaluation is impossible without correcting the measurement system frequency characteristics. In particular, when measuring the error vector magnitude (EVM) of a wideband modulation signal, such as a signal exceeding 10-GHz bandwidth, it is also necessary to calibrate for the phase characteristics as well as for the amplitude characteristics of the down converter. We have tested a system for measuring millimeter-waveband, multi-tone signals using an electro-optic sampling method for the purpose of correcting the phase characteristics of millimeter waveband up converters and down converters. The improved measurement speed and S/N results demonstrate that we achieved our goal of measuring millimeter-wave, three-tone signals in a realistic time.

1 Introduction

The expected huge increase in mobile data traffic is raising questions about how to solve issues in assuring traffic volumes. To meet these requirements, there is increasing demand[1] to use the millimeter wave (mmWave) and terahertz bands for implementing transmission speeds of several gigabits per second (Gbps).

However, presently it is difficult to accurately evaluate wideband signals (DUT signals) in these frequency bands. Although a measurement system can be configured using a down converter, the frequency characteristics of the measurement system, such as the down-converter frequency characteristics, cannot be separated from the measured value. As a consequence, accurate evaluation of the DUT signal is impossible without correction for the measurement system frequency characteristics. In particular, when measuring the error vector magnitude (EVM) of a wideband modulation signal, such as a DUT signal exceeding 10-GHz bandwidth, it is also necessary to correct for the phase characteristics as well as for the amplitude characteristics of the down converter.

Evaluating the characteristics of frequency-conversion devices such as down converters, is difficult using measurement equipment such as network analyzers due to the different frequencies of the input and output ports. As a phase measurement method for up converters and down converters, previously we have used a technique that made assumptions about the mixer reciprocity[3]. However the reciprocity of frequency-conversion devices in the mmWave band is not high, making it difficult to obtain sufficient measurement accuracy. As a result, we examined methods[3, 5] for measuring the phase characteristics of a standalone up converter or a standalone down converter using electro-optic (EO) sampling[2]. This article explains the principles of mmWave phase measurement using EO sampling with some actual test examples and also presents some results with improved measurement speed and S/N ratio for increasing the phase measurement accuracy.

2 Principles of Phase Characteristics Calibration Method

Figure 1 shows the principles of the down-converter phase-characteristics calibration method.

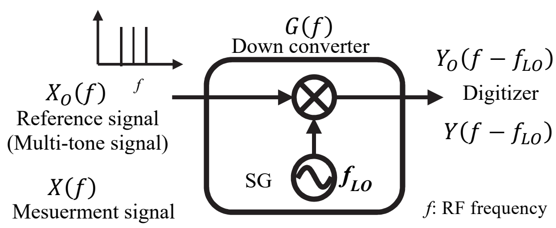

Figure 1 Principles of Phase-Characteristics Calibration

The frequency $G(f)$ of the down converter used in the measurement system can be found from the measured value $Y_O(f - f_{LO})$ in Eq (1) after down conversion using the reference signal $X_O(f)$ where the phase characteristics are known.

$$G(f) = Y_O(f - f_{LO})/X_O(f) \cdots\cdots (1)$$

At evaluation of the Tx signal, the calibrated measured DUT signal $X(f)$ can be obtained using Eq (2) from the value $Y(f - f_{LO})$ measured at input to the down converter and the down-converter frequency characteristics $G(f)$.

$$X(f) = Y(f - f_{LO})/G(f) \cdots\cdots (2)$$

Here, calibrating a modulation signal as the DUT signal with a center frequency of 300 GHz and a bandwidth of 10 GHz requires a reference signal of the same bandwidth, making it extremely difficult to determine the frequency characteristics of a wideband mmWave signal such as this. Consequently, we investigated an EO sampling method to directly measure the frequency characteristics Xo(f) of mmWave and THz-band signals.

3 Principles of Phase Characteristics Measurement

3.1 Electro-Optic Sampling Method

The EO sampling method is based on Pockels effect where the Index of Refraction (IoR) of a medium changes in proportion to the applied electric field strength. Figure 2 shows the structure of an electric field detection system using an electro-optic crystal (EO crystal). In this configuration, a sampling pulse injected to the EO crystal is reflected by a dielectric mirror; the electric field impressed on the EO crystal causes a change in the IoR, changing the polarization of the reflected light. A signal that is proportional to the change in the electric field strength is obtained by converting the change in the polarization condition of the reflected light to an electrical signal. Consequently the field strength can be measured at a specific time by using short optical pulses as sampling pulses.

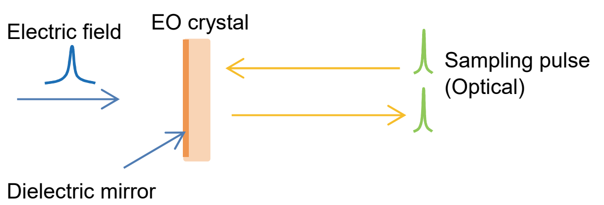

Figure 2 Structure of Field Strength Detector using EO Crystal

Figure 3 (a) shows the block diagram for measuring electrical pulse waves using EO sampling[6]. An electrical pulse is created using a photodiode from the measurement optical pulse synchronized with the sampling optical pulse. Inputting the sampling optical pulse and the electrical pulse to the EO crystal detects changes in the polarization of the reflected light using the polarization detector. The electrical pulse waveform is measured by using a delay line to continuously change the relative timing between the sampling optical pulse and electrical pulse injected to the EO crystal. Figure 3 (b) shows the timing chart for the electrical pulse, sampling optical pulse, and sampled signal when the delay line delay is Δt[7]. Figure 3 (c) shows the reproduced measured waveform when the sampling optical pulse is delayed by Δt_1, $\Delta t_2 \cdots \Delta t_n$ using the delay line.

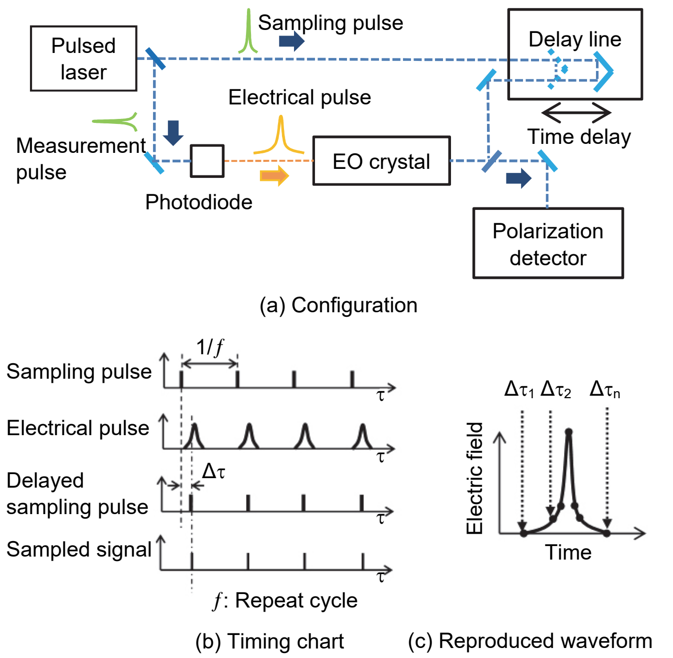

Figure 3 Electrical Pulse Waveform Measurement using EO Sampling

3.2 Measuring Phase Characteristics using Multi-tone Signal

To measure electrical pulses in the time domain using the previously described EO sampling method, we considered how to use these electrical pulses as reference signals for calibrating the down converter. To calibrate the mmWave wide frequency band with high resolution, in addition to shortening the electrical pulse signal pulse width, it is also necessary to lengthen the pulse repetition cycle. However, when inputting a short electrical pulse within the permissible input power range to the down converter, the measurement accuracy tends to be degraded due to the excessively large average power. To solve this problem, we used a multitone signal only in the measured frequency band to prevent the average power from becoming too small. Additionally, since the average power becomes small when the measurement frequency range is wide when the multitone signal covers the entire measured frequency range, we tested a method for obtaining the frequency characteristics for the entire measured frequency range by dividing the multitone signal and measuring the obtained frequency characteristics at each division consecutively.

Figure 4 shows the concept for obtaining the frequency characteristics over the entire measured frequency range by connecting the characteristics obtained from multiple multitone signals. First, we measured a multitone signal in the time domain configured from more than three signals with the same frequency interval using the first EO sampling method. The frequency characteristics were calculated using FFT processing to calculate the phase difference between signals in the multitone signal. After this processing, the same processing was repeated using a multitone signal with changed frequencies so that two or more waveforms overlapped in the multitone signal; the phase frequency characteristics $\varphi(\omega)$ for the entire measured frequency band were calculated by connecting the calculated phase errors.

The following description explains the procedure for calculating $\varphi(\omega)$. First, the phase errors $\Delta\varphi_1$ and $\Delta\varphi_2$ of the three multitone signal shown in Figure 4 (a) were measured. Next, the phase errors $\Delta\varphi'_2$ and $\Delta\varphi'_3$ for f_2, f_3, and f_4 of multitone signal were measured and these were connected. If the relative phase for each sine wave of the multitone signal is undefined, since $\Delta\varphi_2$ and $\Delta\varphi'_2$ are mismatched but $\Delta\varphi_2-\Delta\varphi_1$ and $\Delta\varphi'_3-\Delta\varphi'_2$ are not phase-dependent, $\Delta\varphi$ can be found as the extension of $\Delta\varphi$ from $\Delta\varphi_3 = \Delta\varphi'_3-\Delta\varphi'_2+\Delta\varphi_2$. The phase characteristics for the entire measured frequency band can be obtained by repeating this operation for the desired part of the frequency band as shown in Figure 4 (b).

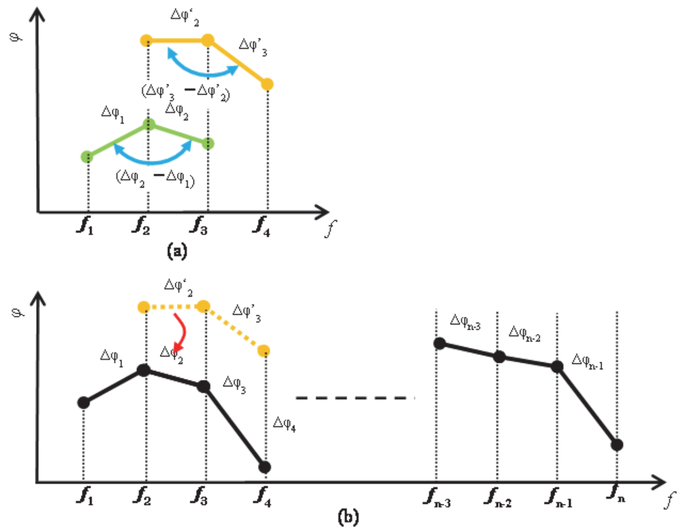

Figure 4 Phase Connection at Acquisition of Frequency Characteristics using Multitone Signal

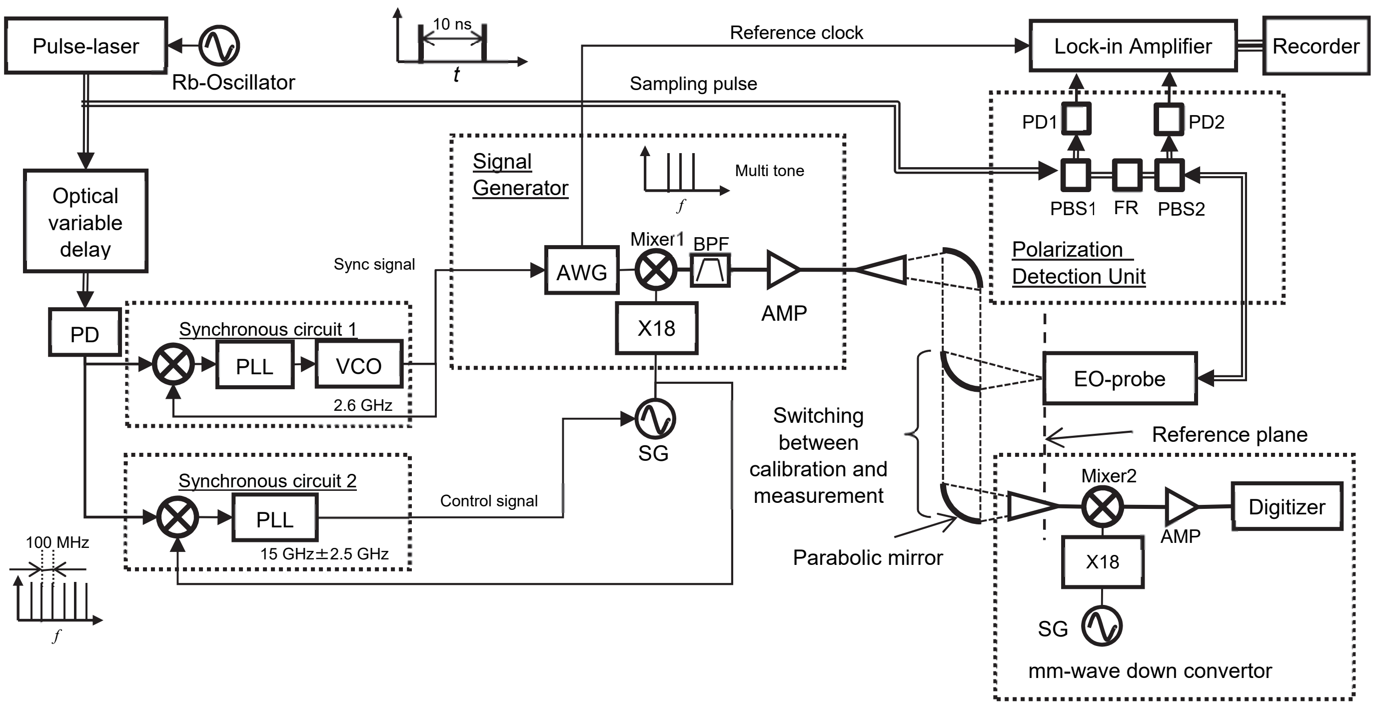

Figure 5 Test Setup for Measuring mmWave 3-Tone Signal using EO Sampling

4 Test Configuration

Figure 5 shows the configuration of the test setup for measuring a 3-tone signal using the EO sampling method composed of a multitone signal-generation section, a field strength measurement section, and a mmWave measurement section.

4.1 Multitone Signal Generator

The mmWave multitone signal generated by the Arbitrary Waveform Generator (AWG) in the Signal Generator is up-converted by Mixer 1 and amplified by the mmWave wideband amplifier.

Since measurement using the EO sampling method requires synchronization of the multitone signal and optical sampling pulse. The AWG and Mixer 1 local signal generator (SG) are synchronized by a short-pulse light source (Pulse laser) with a repetition cycle of 10 ns at Synchronous circuit 1 and 2. The phase of the generated mmWave multitone signal at this time is affected by the synchronization accuracy of the AWG and the Mixer 1 local signal. For example, to hold the phase variation within 10° for 300-GHz signal generation when the synchronization frequency is 100 MHz, the synchronization accuracy must be better than 0.0033° for 1 part in 3000, but this accuracy is difficult to achieve using a phase locked loop (PLL) for the phase comparator. Synchronizing to the nth harmonic component (AWG: 2.6 GHz; SG: 15 ±2.5 GHz) of the Pulse laser repetition frequency (100 MHz) tends to reduce the multitone signal phase variation. Moreover, synchronizing the pulse laser repetition frequency to the rubidium oscillator (Rb oscillator) was designed to cut fluctuations in the repetition frequency. As a result, the frequency variation at an SG output frequency of 15 GHz was reduced from ±4.5 kHz to ±0.45 Hz.

4.2 Field Measurement Section

The Field measurement section measures the generated multitone signal using the EO-probe and Polarization Detection Unit. The EO-probe is composed of an EO crystal with a dielectric mirror sheet at the tip of a polarization-maintaining fiber.

The optical sampling pulse output from the Pulse laser passes via the Polarization Detection Unit and is sent to the EO-probe where the optical sampling pulse with polarization modulated by the electrical field is input to the Polarization Detection Unit backward to the fiber. Here, the polarization components reflected by Polarizing Beam Splitter 2 (PBS2) are input to Photodiode 2 (PD2) for conversion to an electrical signal. The polarization components passing via PBS2 rotate the polarization using the Faraday Rotator (FR) and the components reflected by PBS1 are input to PD1 for conversion to an electrical signal. Performing differential signal detection on the outputs of PD1 and PD2 enables measurement by removing common-mode noise, such as laser intensity noise.

The small Polarization Detection Unit output signal is detected using the Lock-in Amplifier supplied with the external Reference clock to modulate the multitone signal for detection of the same frequency components. Previous systems using mixers were affected by the mixer frequency characteristics, but this configuration uses the AWG features to implement lock-in detection with no effect from mixer frequency characteristics by directly outputting an amplitude-modulated multitone signal. The above-described measurement captures the multitone signal in the time domain while sweeping the Optical variable delay.

5 Improving Measurement Performance

5.1 Improving Measurement Speed

Until now, capture of data from the Lock-in Amplifier used a sequential read method to retrieve data after shifting the Optical variable delay to the desired position. At a resolution of 1 GHz and a frequency band of 500 GHz, about 3000 s are required to measure a multitone signal because about 3 s are required to capture data once in 1-ps steps for a delay shift of 1000 ps. Sixteen measurements are required to measure a 15-GHz bandwidth using a 3-tone signal, resulting in a measurement time of about 48,000 s. Moreover, achieving realistic measurement times is difficult when measuring at higher resolutions. However, the measurement speed was improved by switching from sequential reading from the Lock-in Amplifier to a batch readout method after continuously sweeping the delay.

In concrete terms, the analog output signal of the Lock-in Amplifier when shifting the delay at a constant speed is measured continuously by the Recorder. In this case, the measurement time becomes 500 s for a resolution of 1 GHz and a delay sweep speed of 2 ps/s. Based on high-speed stable delay sweep times of 600 s, this method can shorten previous measurement times by 80%.

Table 1 compares the measurement performance for the different read-out methods and Figure 6 shows the captured spectrums for these methods. Both results are shown for sequential readout and continuous sweeping of a 308-GHz CW signal. Clearly, the continuous sweep method obtains the same spectrum, signal level, floor level, and S/N, as the sequential readout method. However, the measurement time is 80% less for the same S/N, and the S/N is 7 dB better for the same measurement time. When calculating S/N per unit time as an index of measurement performance, the improvement is from −4.51 dB to 2.84 dB.

Table 1 Comparison of Lock-in Amplifier Readout Methods (CW: 308 GHz)

	Signal Level [dB]	Floor Level [dB]	S/N [dB]	Measurement Time [s]	S/N per Unit Time [dB]
Sequential Reading	−142.66	−173.02	30.36	3070	−4.51
Batch Read After Continuous Sweeping	−141.63	−172.25	30.62	600	2.84

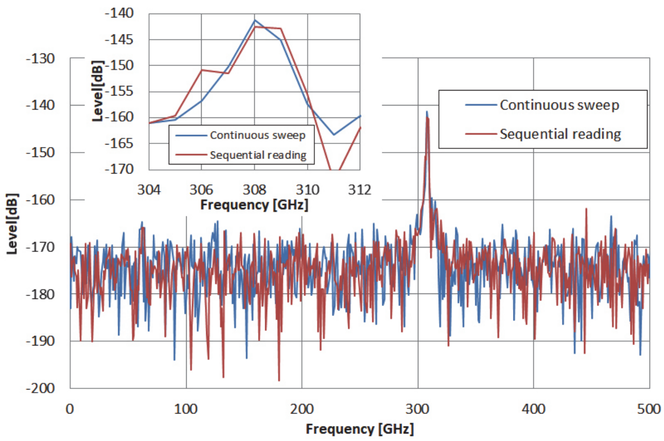

Figure 6 Comparison of Lock-in Amplifier Readout Spectrum Results

5.2 Correction of Delay Differential Linearity

At waveform measurement by sweeping the delay, deviation in the sweep speed is a factor causing drift in the measured frequency. Additionally, the delay differential linearity causes frequency variation. Consequently, the delay sweep speed deviation and differential linearity must be corrected. Therefore, the sweep speed deviation and delay differential linearity for this correction were calculated from the deviation from the ideal value when measuring the time-domain waveform of the CW signal multiple times. Table 2 lists the CW signal measurement results with delay correction enabled and disabled; Figure 7 shows the spectrum.

Table 2 Comparison of Delay Device Correction (CW: 308 GHz)

	Signal Level [dB]	Floor Level [dB]	S/N [dB]	Measurement Time [s]	S/N per Unit Time [dB]
Without Correction	−141.63	−172.25	30.62	600	2.84
With Correction	−138.96	−172.21	33.25	600	5.47

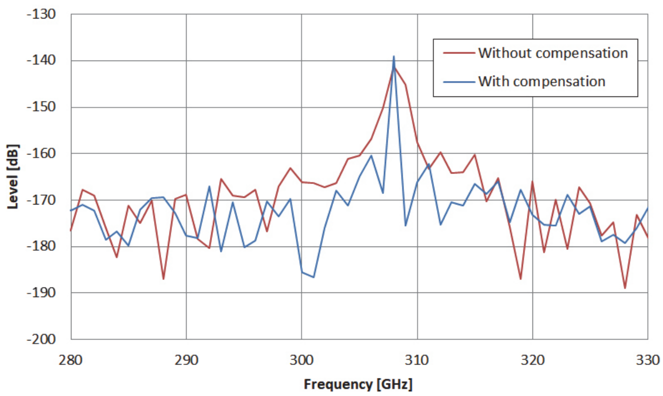

Figure 7 Comparison of Delay Device Correction Spectrums

The S/N of the corrected delay was improved by 2.63 dB. Since the floor level difference was 0.04 dB, the peak level is clearly improved by the delay correction. This is thought to be due to the convergence of the signal components scattered in the frequency region as a result of the delay differential linearity to near the center frequency, and can be confirmed by the sharp spectrum peak.

5.3 Improving S/N

Improving the phase measurement accuracy requires improving the S/N. To measure with minimum noise impact, we re-examined the Lock-in Amplifier reference-clock frequency. Figure 8 shows the Polarization Detection Unit PD output noise characteristics. From these characteristics, there is clearly relatively large noise around 300 kHz, but the noise decreases gently thereafter. Since the Lock-in Amplifier reference clock has an upper frequency limit of 3 MHz, choosing as high as possible frequencies between 300 kHz and 3 MHz enables measurement with minimum noise impact. Table 3 lists the measurement results when the reference clock was revised from 20 kHz to 2.5 MHz and Figure 9 shows the obtained spectrum. From these results, changing the reference clock to 2.5 MHz improved the floor level and as well as the S/N by 11.5 dB.

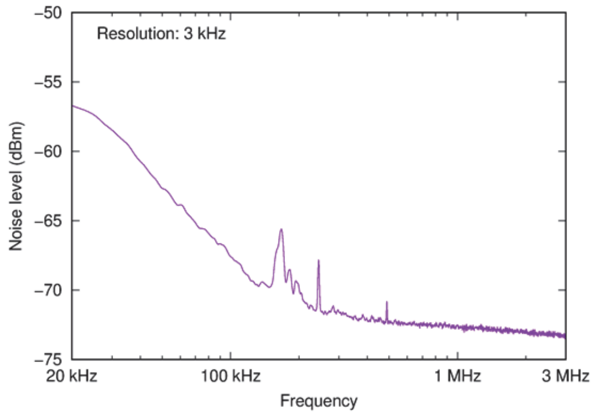

Figure 8 PD Output Noise Characteristics

Table 3 Comparison of Reference Clocks (CW: 308 GHz)

Reference Clock Frequency [MHz]	Signal Level [dB]	Floor Level [dB]	S/N [dB]	Measurement Time [s]	S/N per Unit Time [dB]
0.020	−138.96	−172.21	33.25	600	5.47
2.5	−139.80	−184.55	44.75	600	16.97

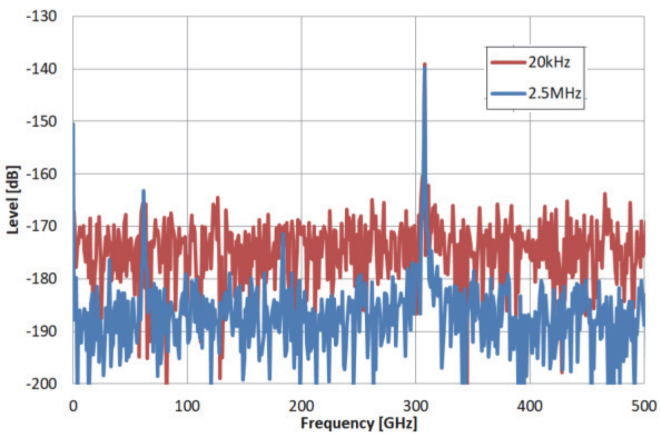

Figure 9 Comparison of Spectrums using Reference Clock Frequency

From the above, combining the faster measurement time acquired by continuous sweeping with delay sweep speed correction improved the S/N per unit time (as an index for evaluating measurement performance) by about 21 dB.

6 Conclusions

This article explains the principles of mmWave 3-tone signal phase measurement using EO sampling as a technology for measuring the phase characteristics of mmWave band frequency converters. As well as explaining the test setup, it also describes improvements to the measurement speed and S/N to improve phase measurement accuracy. As a result, the measurement time for a 15-GHz band was cut from 48,000 seconds to 9600 seconds, and the S/N was improved from 30.36 dB to 44.75 dB. The S/N per unit time (as an index for evaluating measurement performance) was improved from −4.51 dB to 16.97 dB.

These results demonstrate that we achieved our aim of measuring a mmWave three-tone signal in a realistic time.

Acknowledgments

This research was supported by a grant for expansion of electrical waveform frequencies from the Ministry of Internal Affairs and Communications. We thank the committee members for their valuable comments and discussions.

References

1) Tadao Nagatsuma, "Terahertz Technologies Accelerating towards Practical Applications", Journal of the IEICE vol. 97, No. 11, pp. 918-923, Nov. 2014. (in Japanese)

2) D Williams, P Hale, K Remley, "The Sampling Oscilloscope as a Microwave Instrument", IEEE Microwave Magazine, pp. 59-68, Aug. 2007.

3) Y. Kimura M. Fuse S. Mattori and T. Mori, "Study of phase calibration system of Millimeter-wave Down-converter by electro-optics sampling", The Papers of Technical Meeting on Instrumentation and Measurement, IEE-Japan, LAV-17-009 IM—17—009, pp. 49-54 Feb. 2017 (in Japanese)

4) Y. Kimura M. Fuse S. Mattori and T. Mori, "Evaluation of Amplitude Characteristics by Phase Calibration System for Millimeter Wave Downconverter using Electro-optic Sampling Methode", The Papers of Technical Meeting on Instrumentation and Measurement, IEE-Japan, LAV-18-009 IM-18-009, pp. 41-45, Feb. 2018 (in Japanese)

5) Y. Kimura M. Fuse S. Mattori and T. Mori, "Study of Phase Calibration Method of Terahertz-wave Down-converter by Electro-optic Sampling", Proceedings of the 2018 IEICE General Conference, BCI-1-7, Mar. 2018 (in Japanease)

6) D.F. Williams, P.D. Hale, T.S. Clement, and J.M. Morgan, “Mismatch corrections for electro-optic sampling systems”, in Automatic RF Techniques Group Conf. Dig., vol. 56, pp. 141–145, Nov. 2000.

7) T. Yasui, “Speeding-up THz Spectroscopy”, 2007 Symposium on THz Spectroscopy, November 2007. (In Japanese)

Authors

Yukiyasu Kimura
Advanced Technology Development Center
Technical Headquates

Takashi Mori
Advanced Technology Development Center
Technical Headquates

Masaaki Fuse
Advanced Technology Development Center
Technical Headquates

Shigenori Mattori
Advanced Technology Development Center
Technical Headquates